International Journal of Microwave and Wireless Technologies

cambridge.org/mrf

High gain dual-band distributed amplifier using new composite right/left-handed transmission line

Hamed Shahraki[1], Ahmad Hakimi[1], Kambiz Afrooz[1] and Mohammad Mahdi Pezhman[2]

[1]Department of Electrical Engineering, Shahid Bahonar University of Kerman, Kerman, Iran and [2]Department of Electrical Engineering, Yazd University, Yazd, Iran

Research Paper

Cite this article: Shahraki H, Hakimi A, Afrooz K, Pezhman MM (2018). High gain dual-band distributed amplifier using new composite right/left-handed transmission line. *International Journal of Microwave and Wireless Technologies* **10**, 1118–1127. https://doi.org/10.1017/S1759078718001265

Received: 2 February 2018
Revised: 27 July 2018
Accepted: 8 August 2018
First published online: 4 October 2018

Keywords:
Composite right/left-handed (CRLH); dual-band distributed amplifier (DBDA)

Author for correspondence: Kambiz Afrooz, E-mail: Afrooz@uk.ac.ir

Abstract

In this paper, a high-gain dual-band distributed amplifier (DBDA) based on the metamaterial transmission line (TL) is proposed. To have two separate frequency bands in the distributed amplifiers, the composite right/left-handed (CRLH) TLs are used instead of conventional TLs. Although both forward and reverse gains of the distributed amplifiers are available in this case, they suffer from their low gains. In this paper, to increase the DBDA power gain, a new circuit architecture for the CRLH TL is introduced. By using the proposed CRLH TL, a lower wave attenuation coefficient at the forward band of the DBDA is achieved than the conventional structures, which causes a higher forward power gain. Simulation results also show that the power gain of the proposed DBDA is about 28.5 dB at the desired frequency bands, and good agreement between the measurement and simulation results confirms the accuracy of the design method.

Introduction

Multi-band wireless systems have attracted much attention, because of their abilities to work at various standards [1, 2]. There are many applications for multi-band systems such as long-term evolution, global system for mobile communications, and wireless local area network [1]. Accordingly, the demand for an efficient design method to realize multi-band amplifiers is very high. In this regard, dual-band amplifiers have been proposed by using the active feedback circuit technique [3] and switches [4]. Recently, a new technique to design the dual-band circuits and systems has been devised by introducing the metamaterial transmission lines (MTM TL). The MTM TLs have special characteristics such as negative refractive index and nonlinear phase constant that can be used to achieve the various frequency responses [5]. The composite right/left handed (CRLH) TL is the most famous structure of the MTM, which is widely used in the microwave and RF circuits [6, 7]. Several dual-band distributed amplifiers (DBDAs) using the CRLH TL were reported in 2006 [8, 9]. Although this kind of DBDAs has two interesting frequency bands, its power gains are very low [8, 9], which is similar to the conventional DAs. To improve the distributed amplifier (DA) gain, some methods such as cascaded gain cells [10–12] and negative capacitor [13] have been introduced. However, all published multi-band DAs have low power gains [2, 8, 9].

In this work, a new technique to overcome the drawback of low power gain of the DBDAs is introduced. In the proposed technique, a detailed analysis for the wave attenuation coefficients of the conventional DBDAs is first provided. Then, a new unit-cell to decrease the attenuation coefficients, at a desired band is introduced. This leads to a higher power gain for the modified DBDA. It should be noted that although the new CRLH unit-cell can only increase the power gain at the forward band, in addition, by using the obtained analysis, the DBDA power gain can be increased at the other bands by another unit-cell, and a true design. To validate the results, a pHEMT DA based on the CRLH TLs is manufactured and measured. The proposed circuit exhibits a reverse power gain of 28.5 ± 1.5 dB with 2 GHz bandwidth and a forward power gain of 28.5 ± 1.2 dB with 2.5 GHz bandwidth. Furthermore, the simulation results show that the forward power gain of the DBDA is increased about 3 dB, using the introduced CRLH TL. The paper is organized as follows: The DBDA operation mechanism is given in the section "Analysis of DAs". In the next section, the design procedure of the proposed DBDA is illustrated. In the section "Analysis of attenuation coefficient", the theoretical analysis of the attenuation coefficient is given, and the simulation and measurement results are presented in the section "Simulation and measurement results". Finally, concluding remarks are given in the section "Conclusion".

© Cambridge University Press and the European Microwave Association 2018

CAMBRIDGE UNIVERSITY PRESS

Analysis of DAs

Conventional DAs

With reference to the equivalent circuit shown in Fig. 1, a classic DA consists of the cascading active devices and TLs. The forward (G_{fwd}) and reverse (G_{rev}) power gains of the DAs are defined as (1) and (2), respectively, [14–16].

$$G_{fwd} = \frac{P_{fwd}}{P_{in}} = \frac{g_m^2 z_{0g} z_{0d}}{4} \left(\frac{\sin \frac{n}{2}(\beta_g - \beta_d)}{\sin \frac{1}{2}(\beta_g - \beta_d)} \right)^2, \quad (1)$$

$$G_{rev} = \frac{P_{rev}}{P_{in}} = \frac{g_m^2 z_{0g} z_{0d}}{4} \left(\frac{\sin \frac{n}{2}(\beta_g + \beta_d)}{\sin \frac{1}{2}(\beta_g + \beta_d)} \right)^2, \quad (2)$$

where Z_{0g} and Z_{0d} are the characteristic impedances of gate and drain lines, respectively, g_m is the transconductance, β_g and β_d are the phase constants of the gate and drain lines, respectively, and "n" indicates the number of gain cells. It should be noted that these relations are obtained when the transistors are unilateral. Equation (1) shows that, the forward power gain (G_{fwd}) becomes frequency-independent when $\beta_d = \beta_g$. Whereas, according to (2), the reverse power gain (G_{rev}) is frequency-independent when $\beta_d = -\beta_g$. In the conventional DAs, gate and drain TLs are right-handed (RH) (shown in Fig. 2(a)), which the phase constant of this TL, is given by (3).

$$\beta_{RH} = \omega \sqrt{L_g C_g}. \quad (3)$$

From (3), β is always positive and therefore, only the forward power gain (S_{41}) of the conventional DA is usable. This condition can be changed by replacing the RH TL with the CRLH TL.

CRLH TL

Figure 2(b) shows the equivalent circuit of a CRLH TL. The CRLH TL consists of a series LC resonator (Z_d) in the horizontal branch and a parallel LC resonator (Y_d) in the vertical branch. The phase constant of the CRLH TL can be obtained as follows [17]:

$$\beta = s(\omega) \sqrt{\left(\omega C_R - \frac{1}{\omega L_L} \right) \times \left(\omega L_R - \frac{1}{\omega C_L} \right)}, \quad (4)$$

where $s(\omega)$ is the following:

$$s(\omega) = \begin{cases} -1 & \text{if} \quad \omega \le \min(\omega_{se} = 1/\sqrt{C_R L_L},\ \omega_{sh} \\ & = 1/\sqrt{C_L L_R}\ ) \quad \text{LHrange} \\ +1 & \text{if} \quad \omega \ge \max(\omega_{se} = 1/\sqrt{C_R L_L},\ \omega_{sh} \\ & = 1/\sqrt{C_L L_R}\ ) \quad \text{RHrange.} \end{cases}$$

DBDA with CRLH TL

Equation (4) shows that unlike the RH TLs, the CRLH TLs can have $\beta < 0$. Therefore, by replacing the RH TL with the CRLH TL in a DA, the situations of $-\beta_d = \beta_g$ and $\beta_d = \beta_g$ could be achieved at two various frequencies, respectively [9]. As a result, both forward and reverse gains could be frequency-independent.

Design of the DBDA

The main structure of the proposed DBDA is illustrated in Fig. 3. Port 1 and Port 2 are the input and isolated ports, respectively, and Port 3 and Port 4 are the output ports. This structure amplifies the input signals at two various frequency bands, with center frequencies of f_1 and f_2 and then extracts them from Ports 3 and 4, respectively.

Design of the TLs

As shown in Fig. (3), the gate and drain lines of the proposed DBDA are provided by the RH and CRLH TLs, respectively. There are two reasons for these choices: First, by selecting the CRLH TL as the gate line, it has the significant effects and distortions on the return loss (S_{11}), therefore, the RH TL is selected as the gate line. Second, by increasing the number of gain cells (longer gate TL), the wave attenuation of the gate line increases and finally, it can surpass the amplification. Thus, the number of gain cells is limited by the attenuation of the gate line. As a result, since the RH TL has the lower attenuation than the artificial TL [5], it should be selected as the gate line.

To design the TLs, first, the desired frequency ranges for the forward (f_2) and reverse (f_1) power gains should be determined.

There are two points to note about f_1 and f_2 frequencies:

(i) In fact, by a suitable approximation, f_1 and f_2 are the center frequencies of the reverse and forward bands and therefore these frequencies must be carefully selected. However, parasitic elements and transistor model errors can change this issue.
(ii) It should be noted that by increasing the value of f_2 than f_1, the wider frequency bands for the DBDA are obtained.

But the proposed DBDA is designed by using ATF36-163 HEMT transistor, that its gain decreases after 10 GHz, severely. Then $f_1 = 4$ GHz and $f_2 = 8$ GHz are selected. It is clear that by using the transistors with higher f_t, achieving a higher f_2 and accordingly a wider bandwidth is possible.

From (5), the RH TLs are fully determined by their matching conditions and phase specifications, at a single operating frequency [5].

$$\begin{cases} C_g = \beta_1 / \omega_1 Z_{0C} \\ L_g = Z_{0C}^2 C_g \end{cases}, \quad (5)$$

where Z_{0C} is the characteristic impendence, and is selected equal to the port impedance (50 Ω), to achieve a wide band matching [5]. In addition, the phase constant of the RH TL is a linear function of frequency (Eq. (5)). Therefore, the whole dispersion curve is determined by having the value of β at a specified frequency. On the other hand, unlike the RH TLs, CRLH TLs have four elements in their circuit models (instead of two), and their dispersion curves are nonlinear. Therefore, designers have a greater degree of freedom. Hence, the design procedure is started by designing a RH TL as the gate line. In this regard, an arbitrary value for $\beta_g(f_1)$ should be selected. In this paper, it is assumed

https://doi.org/10.1017/S1759078718001265 Published online by Cambridge University Press

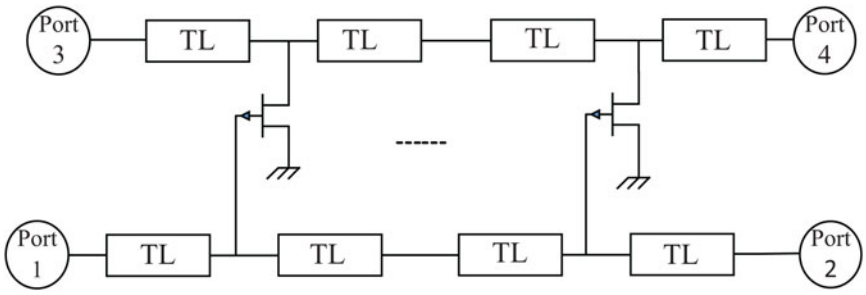


Fig. 1. Conventional distributed amplifier.

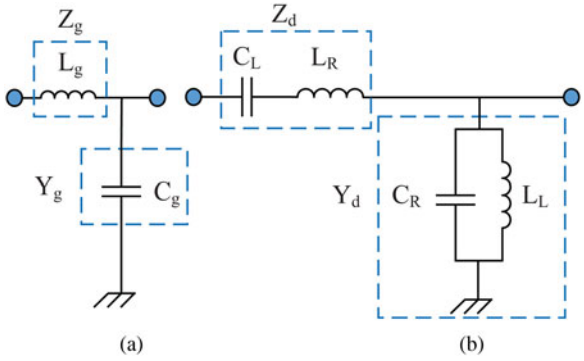


Fig. 2. (a) RH and (b) CRLH unit cell.

that $\beta_g(4\ \text{GHz}) = 0.65$ (rad/m). From (3), β_g equals 1.3 (rad/m) at 8 GHz frequency. As a result, to achieve the DBDA, a CRLH TL should be designed as the drain line, such that the following conditions are satisfied:

$$\begin{aligned} \beta_d(4\,\text{GHz}) &= -0.65(\text{rad/m}) \quad \text{and} \\ \beta_d(8\,\text{GHz}) &= 1.3\,(\text{rad/m}). \end{aligned} \tag{6}$$

The components values of the CRLH unit-cell can be obtained as below [5]:

$$\begin{cases} C_R = (\beta_1\omega_1 - \beta_2\omega_2)/(Z_{0C}(\omega_1^2 - \omega_2^2)) \\ C_L = 1/\left(\omega_1^2 - \dfrac{\beta_1\omega_1}{Z_{0C}C_R}\right)Z_{0C}^2C_R \\ L_R = Z_{0C}^2C_R \\ L_L = Z_{0C}^2C_L, \end{cases} \tag{7}$$

where Z_{0C} is the characteristic impedance, and is selected equal to the port impedance (50Ω) to achieve a wide band matching [5]. Table 1 shows the calculated element values of TLs, using (5)–(7). According to the given values in Table 1, the dispersion curves of the gate and drain lines are plotted in Fig. 4. As shown in the figure, the phase constants of the gate and drain TLs are the same at two frequencies of 4 GHz and 8 GHz. Therefore, the design procedure of TLs to achieve a DBDA is completed.

Overall structure of the proposed DBDA

As mentioned previously, DAs have a broad bandwidth while their gains are low, due to the additive gain mechanism [1]. In recent years, to solve the low gain problem of DAs, many topologies have been reported, such as cascaded single stage DAs (CSSDA) [1] and matrix DAs [18], which their gain mechanisms are multiplicative. Therefore, to realize a high-gain DBDA, the proposed structure is designed based on the multiplicative gain mechanism, as the first step. As shown in Fig. 3, the gain cell is realized by two cascaded common-source transistors. Simulation of the designed DBDA is performed using the ADS simulator. The results are shown in Fig. 5, and the proposed DBDA achieves a forward power gain (S_{41}) of 24.5 ± 1 dB, and a reverse power gain (S_{31}) of 27.5 ± 1. Although the designed structure has a high power gain compared with the other reported multi-band DAs [2, 8, 9], the forward power gain is about 3 dB lower than the reverse power gain. This issue can be related to the increase of the parasitic effects with frequency. In the section "Analysis of attenuation coefficient", to reduce the power gain difference between S_{31} and S_{41} of the introduced DBDA and to increase the power gain at the forward band, a new method is presented.

Analysis of attenuation coefficient

Preliminary

In the general case, with the bilateral ($S_{12T} \neq 0$) transistors, the wave propagation constants of drain and gate lines have a positive real part, even when transmission lines are lossless [19]. In this work, by decreasing the wave attenuation coefficient in the proposed DBDA, its power gain at the forward band is enhanced. To provide insight, the attenuation coefficients of the conventional DBDAs were first calculated and then compared with the proposed DBDA. The equivalent circuit of a small segment of a DA is shown in Fig. 6. Using the voltage and current equations in the drain and gate lines, the voltages in the gate and drain lines can be described by the following system of the linear partial differential equations [19]:

$$\frac{\partial^2}{\partial x^2}\begin{bmatrix} v_g \\ v_d \end{bmatrix} = \begin{bmatrix} A_{11} & A_{12} \\ A_{21} & A_{22} \end{bmatrix}\begin{bmatrix} v_g \\ v_d \end{bmatrix}, \tag{8}$$

where $A_{11} = z_g(y_g + y_{gd})$, $A_{12} = -z_g y_{gd}$, $A_{21} = (g_m - y_{gd})z_d$, and $A_{22} = z_d(y_d + y_{gd})$. In addition, z_g, y_g, z_d, and y_d can be determined from Fig. 2. By applying the Laplace transform on (8), a characteristic equation is derived as below [19]:

$$(S^2 - A_{11})(S^2 - A_{22}) - A_{12}A_{21} = 0, \tag{9}$$

where "S" is the laplace frequency. It should be noted that to present a comprehensive analysis for the attenuation coefficients, the relations of this section are obtained when the transistors are bilateral. Furthermore, the voltage waves in the gate and drain

https://doi.org/10.1017/S1759078718001265 Published online by Cambridge University Press

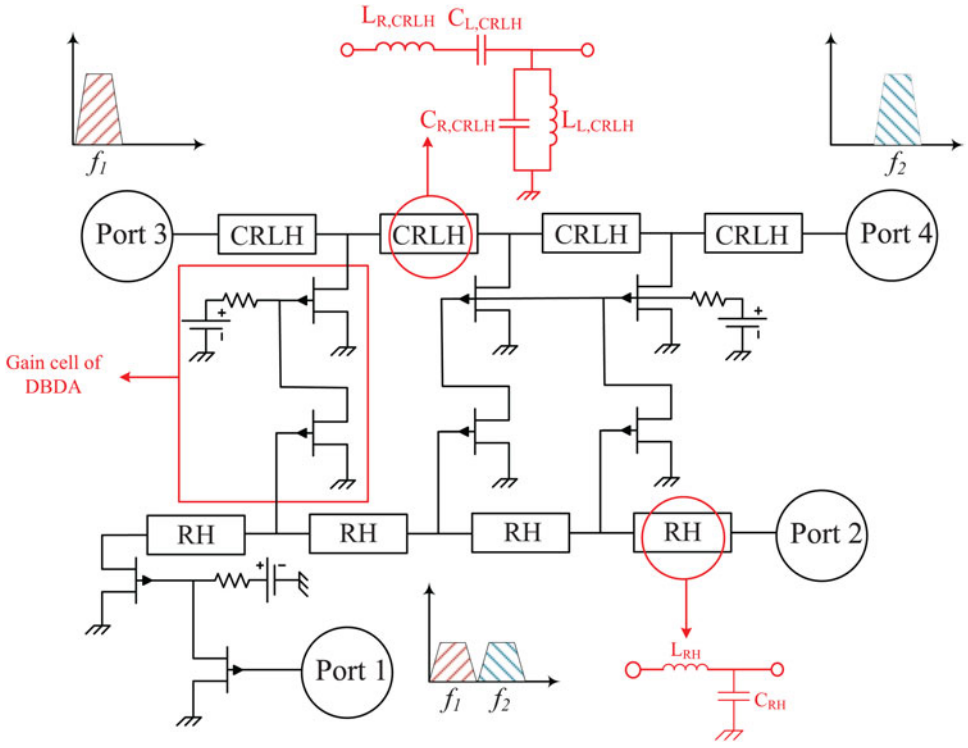


Fig. 3. Schematic of the proposed DBDA.

Table 1. Lumped elements for the TLs

$C_G(PF)$	$C_L(PF)$	$C_R(PF)$	$L_L(nH)$	$L_R(nH)$	$L_G(nH)$
0.5	0.4	0.9	1	2.25	1.25

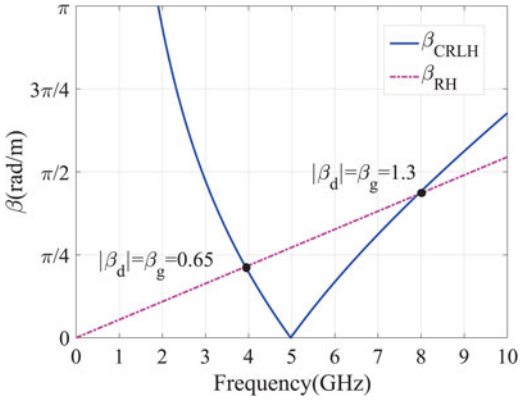


Fig. 4. Dispersion curves of the designed RH (dashed line) and CRLH TLs (solid line).

lines have the general form of (10) [19].

$$V(x) = k_1 e^{-\gamma_1 x} + k_2 e^{\gamma_1 x} + k_3 e^{-\gamma_2 x} + k_4 e^{\gamma_2 x}. \quad (10)$$

Using (8) and (9), the propagation constants of the DA ($\gamma_{1,2}$) are derived as follows [19]:

$$\gamma_{1,2} = \alpha_{1,2} + j\beta_{1,2} = \sqrt{\frac{A \pm \sqrt{B + 4C)}}{2}}, \quad (11)$$

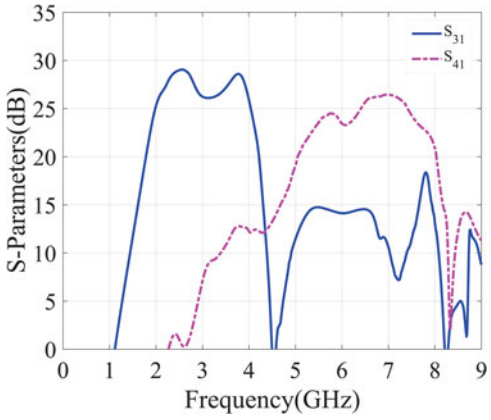


Fig. 5. S-Parameters of the DBDA with the conventional unit-cells.

where $A = A_{11} + A_{22}$, $B = (A_{11} - A_{22})^2$, and $C = A_{12}A_{21}$.

$$A = z_g(y_g + y_{gd}) + z_d(y_d + y_{gd})$$
$$= (j^2\omega^2 L_g C_g') + (j\omega L_r + \frac{1}{j\omega C_l})\left(j\omega C_{gr} + \frac{1}{j\omega L_l}\right)$$
$$B = \left(z_g(y_g + y_{gd}) - z_d(y_d + y_{gd})\right)^2$$
$$= \left((j^2\omega^2 L_g C_g') - \left(j\omega L_r + \frac{1}{j\omega C_l}\right)\left(j\omega C_{gr} + \frac{1}{j\omega L_l}\right)\right)^2$$
$$C = -(g_m - j\omega C_{gd})\left(j\omega L_r + \frac{1}{j\omega C_l}\right)$$
$$\times (j\omega C_{gd} \times j\omega L_g) \text{and} C_g' = C_g + C_{gd}.$$

https://doi.org/10.1017/S1759078718001265 Published online by Cambridge University Press

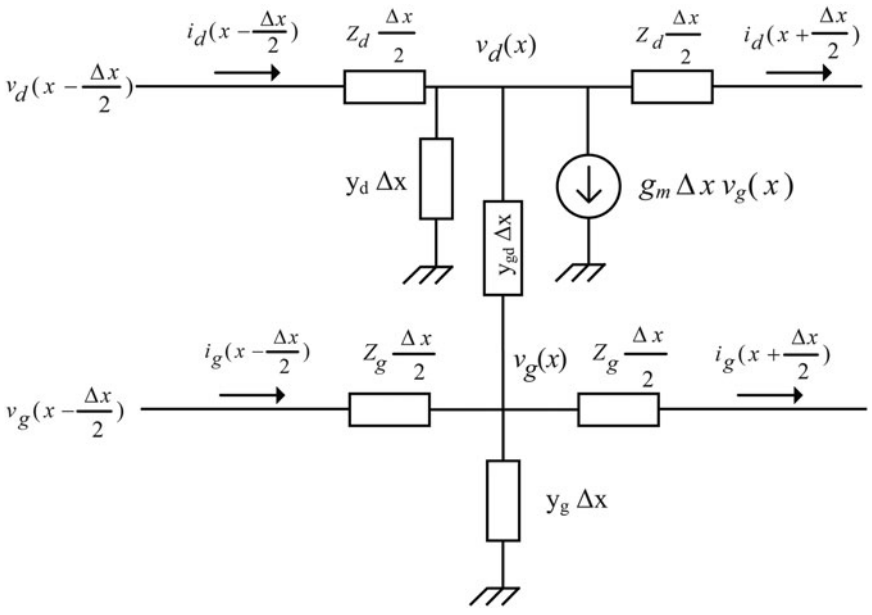


Fig. 6. Equivalent circuit of a small segment of the DA.

The real parts of $\gamma_{1,2}$ (α_1 and α_2), are plotted in Fig. 7. As mentioned previously, the goal of the paper is to decrease the attenuation coefficients at the desired frequency band, which is shown in the rectangular area of Fig. 7. From (11), the attenuation coefficient (α) is minimized when:

$$A \pm \Re e\sqrt{B+4C} < 0 \;\&\; \begin{cases} (1)\; A \pm \Re e(\sqrt{B+4C}) \to -\infty \\ (2) \quad or \quad \mathrm{Im}(\sqrt{B+4C}) \to 0 \end{cases}. \tag{12a}$$

And α is maximized when:

$$A \pm \Re e\sqrt{B+4C} > 0 \;\&\; \begin{cases} (1)\; A \pm \Re e(\sqrt{B+4C}) \to +\infty \\ (2) \quad or \quad \mathrm{Im}(\sqrt{B+4C}) \to 0. \end{cases} \tag{12b}$$

$$\{(3) \quad \mathrm{Im}(\sqrt{B+4C}) \to +\infty \quad \& \; A \pm \Re e(\sqrt{B+4C}) < 0. \tag{12c}$$

The proof of equation (12) is given in appendix A.

Finding the corresponding frequencies to α_{min}

In the case where $A \pm \Re e(\sqrt{B+4C}) \to -\infty$

Equation (12a-1) shows that the attenuation coefficient (α) is minimized when either term "A" or $\Re e(\sqrt{B+4C})$ goes to $-\infty$. In the general case, A and $\Re e(\sqrt{B+4C})$ are always negative and positive, respectively (as will be seen in Fig. 15), and the magnitude of A is always greater than $\Re e(\sqrt{B+4C})$, which guarantees the negative sign for $(A \pm \Re e(\sqrt{B+4C}))$. In other words, to find the corresponding frequencies to $\alpha_{\min}$, the poles of term "A" should be calculated as follows:

$$\begin{aligned} A &= z_g(y_g + y_{gd}) + z_d(y_d + y_{gd}) = (j^2\omega^2 L_g C_g') \\ &\quad + \left(j\omega L_r + \frac{1}{j\omega C_l}\right)\left(j\omega C_r + \frac{1}{j\omega L_l}\right) \\ &= -\infty \Rightarrow z_d y_d = -\infty \Rightarrow \omega_{\alpha_{1,2}\min_1} = 0. \end{aligned} \tag{13}$$

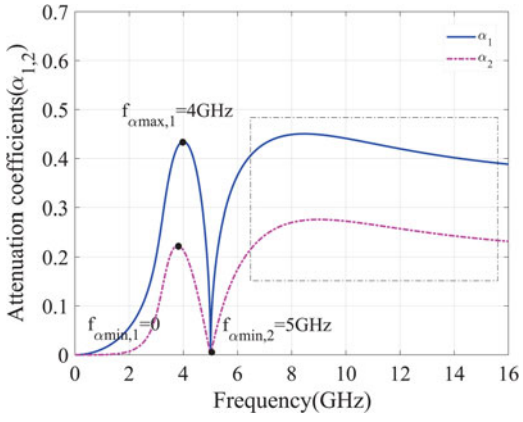


Fig. 7. The attention coefficients of the DBDA (the elements are selected as Table 1).

From (13), since z_g, y_g, and y_{gd} do not have any poles, poles of "A" are the same with Z_d and Y_d (where Z_d and Y_d are the horizontal branch impedance and the vertical branch admittance of the CRLH unit cell, respectively).

In the case where $\mathrm{Im}(\sqrt{B+4C}) \to 0$

In addition, according to (12a-2), the attenuation coefficient (α) is minimized when:

$$\begin{aligned} &\mathrm{Im}(\sqrt{B+4C}) \to 0 \overset{B \text{ is purely real}}{\to} \mathrm{Im}(C) = 0 \\ &\Rightarrow \mathrm{Im}\left[-(g_m - j\omega C_{gd})\left(j\omega L_r + \frac{1}{j\omega C_l}\right) \times (j^2\omega^2 C_{gd} L_g)\right] = 0 \\ &\Rightarrow j\omega L_r + \frac{1}{j\omega C_l} = 0 \Rightarrow \omega_{\alpha_{1,2}\min_2} = \frac{1}{\sqrt{L_r C_l}}. \end{aligned} \tag{14}$$

Thus, in the DBDAs based on the conventional CRLH TL, $\alpha_{1,2}$ are minimized at the zero frequency of the horizontal branch ($\omega_{\alpha\min 2} = (1/\sqrt{L_R C_L})$) and pole frequencies of the horizontal

https://doi.org/10.1017/S1759078718001265 Published online by Cambridge University Press

and vertical branches ($\omega_{\alpha\ \min\ 1} = 0$). As a result, the attenuation coefficient can be decreased at the desired frequency band, by adding a suitable pole to one of the branches (horizontal or vertical) of the CRLH. This goal is achieved by introducing a new CRLH TL.

Adding a new minimum point to α curve, in the Case $A \pm \Re e(\sqrt{B+4C}) \to -\infty$

Figure 8 shows the proposed CRLH unit cell. As shown in the figure, the horizontal branch of the proposed topology is similar to the conventional CRLH TL, but in the vertical branch, a series inductor (L_m) is added to the parallel LC resonator. The attenuation and phase constants of this TL, in comparison with the conventional type, are illustrated in Fig. 9. It is clear that the difference between these two TLs is noticeable, only at the RH band. Hence, it is expected that by using the introduced TL, only S_{41} of the proposed DBDA is changed. From Fig. 8, the admittance of the vertical branch is equal to:

$$Y_{d_{new}} = \frac{1}{j\omega L_m + \dfrac{1}{j\omega C_r + (1/j\omega L_l)}} = \frac{(j^2\omega^2 L_l C_r) + 1}{j\omega(L_m(j^2\omega^2 L_l C_r) + (L_m + L_l))}. \quad (15)$$

According to (15), the vertical branch admittance (Y_{dnew}) of the proposed CRLH TL has two acceptable poles in comparison with the single pole of the conventional CRLH TL. The new pole of Y_{dnew} is obtained as below:

$$Y_{dnew} \to \infty \Rightarrow \frac{(j^2\omega^2 L_l C_r) + 1}{j\omega L_m(j^2\omega^2 L_l C_r) + j\omega L_l} \to \infty \Rightarrow j\omega L_m(j^2\omega^2 L_l C_r) + j\omega L_l = 0 \to \omega_{\alpha_{1,2}\min 3} = \sqrt{\frac{L_l/L_m + 1}{C_r L_l}}. \quad (16)$$

Figure 10 shows the attenuation coefficients for the proposed structure. As expected, using the introduced CRLH, α becomes zero at three frequencies in opposition to the conventional type, which the number of these frequencies is two. It can also be observed that the wave attenuation coefficient is severely decreased at frequencies between $\omega_{\alpha,\min\ 2}$ and $\omega_{\alpha,\min\ 3}$, leading to higher power gain for the structure. From Fig. 11, by using the proposed CRLH, the forward power gain (S_{41}) is increased about 3 dB and the level difference between S_{31} and S_{41} is removed.

Simulation and measurement results

To validate the discussed analysis, a DBDA was designed using the ATF36163 HEMT transistor. It has been fabricated on the RO4003C substrate with the relative permittivity of 3.55, loss tangent equal to 0.0027, and thickness of 0.5 mm. The required series capacitor (C_L) in the CRLH unit cell is provided by the interdigital capacitor, and the capacitance value (C_L) and the inductance value (L_R) (shown in Fig. 2) depend on the number and thickness of the interdigital fingers and their gap width. The output impedance of the active device is used to make the capacitance C_R and inductance L_L. Also, the transmission line between the active devices and the drain TL creates the inductor (L_m) of the proposed CRLH TL. It should be noted that, there are limitations on the realization of TLs:

1) In the general case, since the series capacitance C_L (shown in Fig. 2) is usually provided by an interdigital capacitor, designers have several technological limitations: First, the interdigital capacitor has a poor capacitance per-unit-length, especially at microwave frequencies. Secondly, the bandwidths

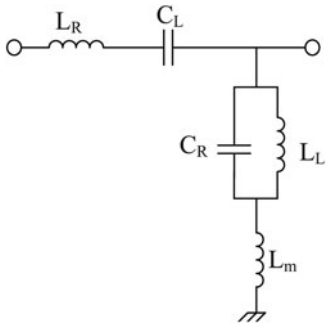


Fig. 8. The proposed CRLH TL.

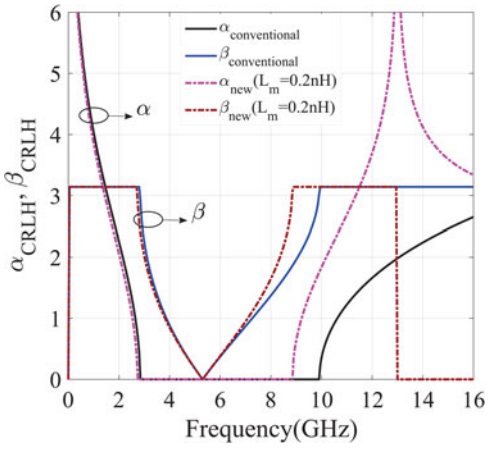


Fig. 9. β and α for the CRLH unit cell.

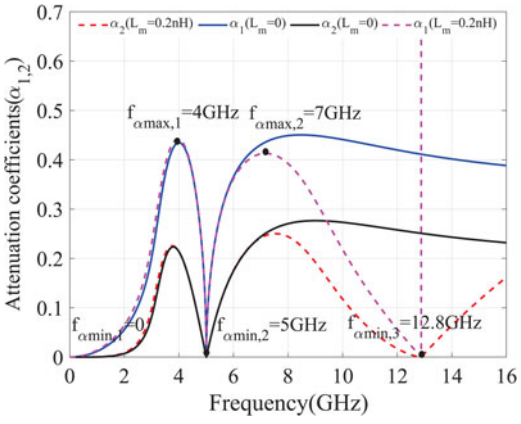


Fig. 10. The attention coefficients of the DBDA (solid lines: using the conventional CRLH TL, dotted lines: using the proposed CRLH TL, $L_m = 0.2$ nH).

https://doi.org/10.1017/S1759078718001265 Published online by Cambridge University Press

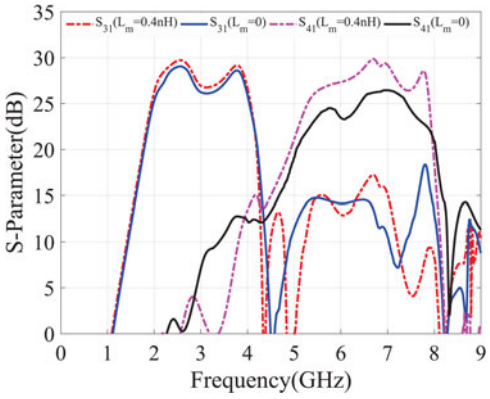


Fig. 11. S-Parameters of the proposed DBDA: using the conventional CRLH TL (solid lines: $L_m = 0$), using the proposed CRLH TL (dashed lines: $L_m = 0.4$ nH).

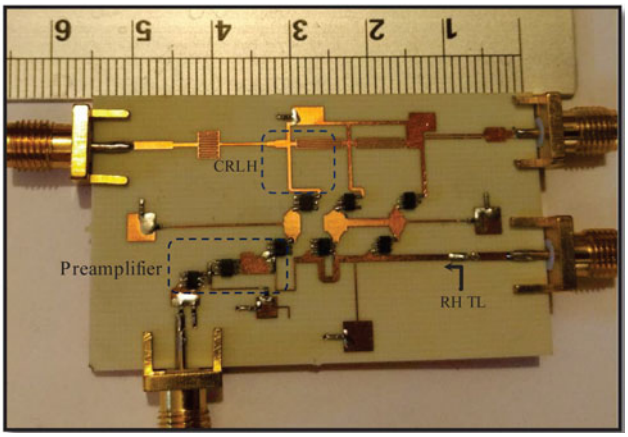


Fig. 12. Photograph of the fabricated DBDA.

of these structures are limited by spurious transverse resonances of the interdigital capacitor. In fact, designers to realize the capacitance higher than 1 PF (using interdigital capacitor) have many problems, due to the imposed spurious transverse resonances. Therefore, there is a minimum operating frequency to choose.

2) On the other hand, the operating frequency cannot be increased to any desired value, since to achieve that, the element values of the metamaterial unit cell should be selected as small as necessary. But this is impossible, because of the parasitic elements of the active devices (which play an important role to realize these unit cells) cannot be reduced to the extent necessary. Therefore, according to the used technology, there is a maximum frequency to choose.

The transistors were biased at $V_{\text{drain}} = 1.3$ V, $V_{\text{source}} = 0$ V, $V_{\text{gate}} = 0.2$ V. The total drain current for transistors was 40 mA, and for DC bias, the lumped discrete capacitors (100 pF) were utilized as dc blocks in several points on the board. Figure 12 shows the photograph of the fabricated circuit, which its total chip area is 17.5 (3 cm × 5.5 cm). As shown in the figure, the proposed DBDA is composed of two main parts:

1) A CSSDA is attached to the input port which includes two cascaded transistors and an input matching circuit. There are two reasons for adding this part to the proposed structure: when the pre-amplifier is removed, the gate TL is responsible for the input matching. Furthermore, as said before, to provide a DBDA, the gate and drain TLs should be designed such that condition (6) is satisfied. As a result, there are some problems to achieve the input matching and condition (6), simultaneously. By adding the preamplifier, the isolation between the input port and the gate line is improved. Hence, easier access to the input matching at the wide bandwidth and a greater degree of freedom to design the gate line are achieved.
2) A common DA, in which the drain TL was constructed by the CRLH TL and converts the DA into the DBDA. The gain cell of this part was formed by two cascaded common-source transistors.

To provide insight, the preamplifier and the DBDA parts are simulated separately, and the results are shown in Fig. 13. As

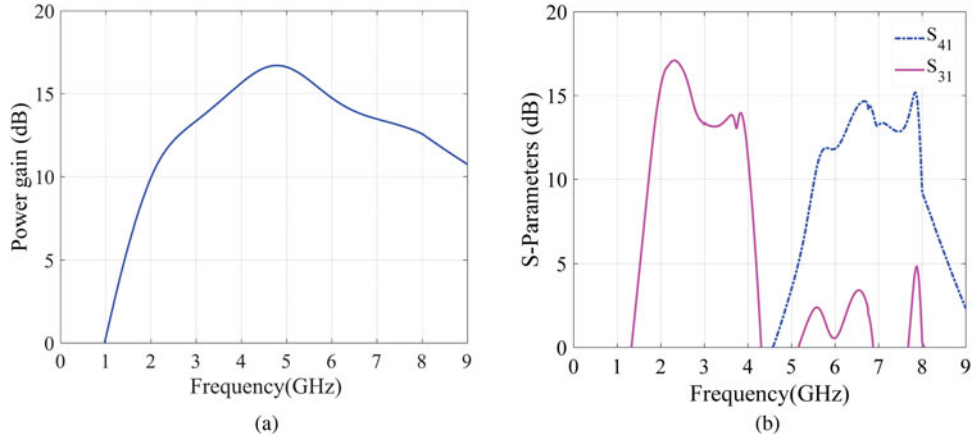


Fig. 13. The power gains of the (a) preamplifier, (b) DBDA part.

https://doi.org/10.1017/S1759078718001265 Published online by Cambridge University Press

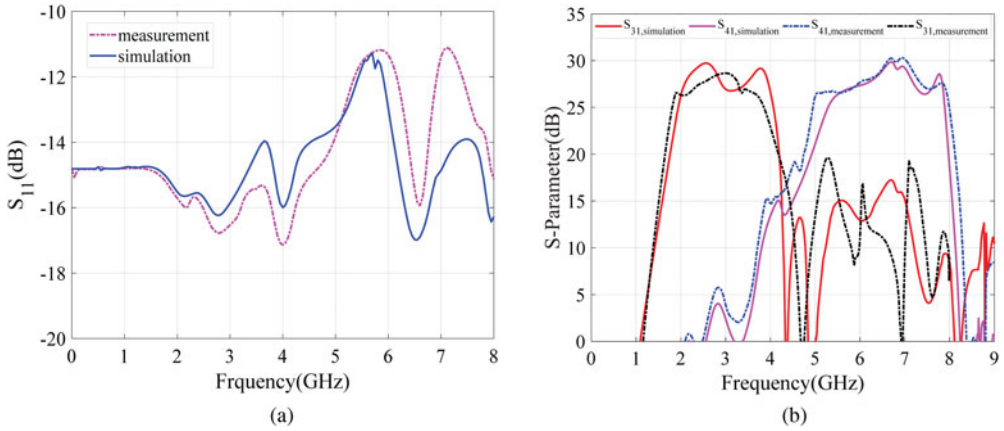


Fig. 14. S-parameters of the DBDA: (a) S_{11} and (b) power gains of the proposed DBDA (solid lines: full-wave simulation, dotted lines: measurement).

Table 2. Comparison of the results for multi-band DAs.

Ref	Amplifier	Technology	Num. of outputs	Frequency	Power gain	S_{11}(dB)
[2]	DA	pHEMT(ECRLH)	2 (quad band)	2.6 – 3.2(0.6 GHz) 4 – 4.5(0.5 GHz) 2.25 – 2.6(0.35 GHz)	8–11	–10
[8]	MDA	FET(CRLH)Active Coupling	2 (dual band)	3.25 – 3.75(0.5 GHz) 0.35 – 0.65(0.3 GHz) 0.6 – 0.7(0.1 GHz)	5–9	–
[16]	DA	GaAs MESFET(CRLH)	2 (dual band)	1.4 – 2.4(1 GHz) 2.5 – 4(1.5 GHz)	6–10	–6
[20]	DA	HEMT (CRLH)	2 (dual band)	1.3 – 1.8(0.5 GHz) 2 – 3.5(1.5, GHz)	18–20	–10
[21]	DA	MMIC 0.15 um HEMT(CRLH)	2 (dual band)	9 – 10.5(1.5 GHz) 11.8 – 12.4(0.6 GHz)	10–12	–20
This work	DA (without pre-amplifier)	HEMT(CRLH)	2 (dual band)	2 – 4(2 GHz) 5.5 – 8(2.5 GHz)	13–15	–
This work	DA (with pre-amplifier)	HEMT(CRLH)	2 (dual band)	2 – 4(2 GHz) 5.5 – 8(2.5 GHz)	27–30	–11.3

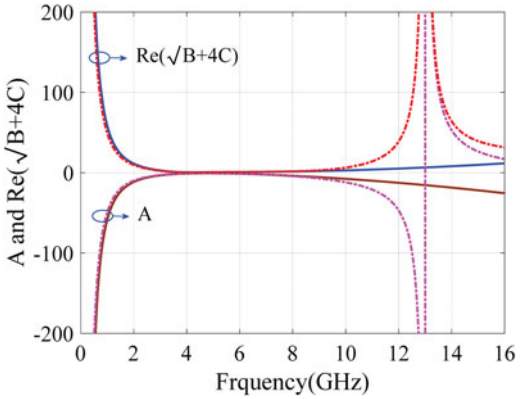


Fig. 15. The variation of terms "A" and real($\sqrt{B+C}$) versus frequency using: (Solid lines: $L_m = 0$, dotted lines: $L_m = 0.2$ nH).

illustrated, the preamplifier has a power gain of 12.5 dB, and therefore it plays an important role in improving the power gain. Furthermore, the DBDA part by having the forward and reverse power gains of 13 dB provides a dual band amplifier.

The scattering parameters of the DBDA are plotted in Fig. 14. From Fig. 14(a), the return loss (S_{11}) of the designed DBDA is better than 10 dB through the forward and reverse frequency bands. As shown in Fig. 14(b), the DBDA achieves 28.5 ± 1.2 dB forward gain (S_{41}) and 28.5 ± 1.5 dB backward gain (S_{31}). In addition, the 3-dB bandwidths of the forward and backward power gains are 2.5 GHz (from 5.5 to 8 GHz) and 2 GHz (from 2 to 4 GHz), respectively. The obtained bandwidth is good in comparison with the conventional DBDAs. In addition, simulated and measured results show an acceptable agreement. Some reported multi-band DAs are presented in Table 2, for comparison. It is clear that the proposed circuit has a higher power gain and wider bandwidth, than the other reported DBDAs.

Conclusion

A high-gain dual-band DA with composite right/left-handed transmission line has been presented. By using a new CRLH TL in the DBDA, the attenuation coefficients have decreased, leading to increased S_{41} for the structure, (about 3 dB at high-frequency band). The proposed method can be used to increase the power

https://doi.org/10.1017/S1759078718001265 Published online by Cambridge University Press

gain of the DAs or other active circuits which use the metamaterial TL. The proposed circuit exhibits 28.2 dB reverse gain with a bandwidth of 2 GHz and 28.5 dB forward gain with a bandwidth of 2.5 GHz.

Acknowledgments. The authors would like to thank Iranshahr Velayat University for help and support with measurements.

References

1. **Mohammadi A and Ghannouchi FM** (2012) *RF Transceiver Design for MIMO Wireless Communications*. Heidelberg, Germany: Springer Science & Business Media.
2. **Keshavarz R, Mohammadi A and Abdipour A** (2013) A quad-band distributed amplifier with E-CRLH transmission line. *IEEE Transactions on Microwave Theory and Techniques* **61**, 4188–4194.
3. **Yamamoto K and *et al.*** (2000) A 3.2-V operation single-chip dual-band AlGaAs/GaAs HBT MMIC power amplifier with active feedback circuit technique. *IEEE Journal of Solid-State Circuits* **35**, 1109–1120.
4. **Fukuda A, Okazaki H, Hirota T and Yamao Y** (2004) Novel 900 MHz/1.9 GHz dual-mode power amplifier employing MEMS switches for optimum matching. *IEEE Microwave and Wireless Components Letters* **14**, 121–123.
5. **Caloz C and Itoh T** (2005) *Electromagnetic metamaterials: transmission line theory and microwave applications*. Hoboken, NJ, USA: John Wiley & Sons.
6. **Hu X** (2009) *Some studies on metamaterial transmission lines and their applications* (Ph.D. thesis). KTH.
7. **Caloz C and Itoh T** (2003) *Novel microwave devices and structures based on the transmission line approach of meta-materials, in Microwave Symposium Digest, 2003 IEEE MTT-S International, June*. pp. 195–198.
8. **Mata-Contreras J, Martin-Guerrero T and Camacho-Penalosa C** (2007) *Experimental performance of a meta-distributed amplifier, in Microwave Conference, European, IEEE, June*. pp. 743–746.
9. **Mata-Contreras J, Martin-Guerrero T and Camacho-Penalosa C** (2006) Distributed amplifiers with composite left/right-handed transmission lines. *Microwave and Optical Technology Letters* **48**, 609–613.
10. **Arbabian A and Niknejad AM** (2009) Design of a CMOS tapered cascaded multistage distributed amplifier. *IEEE Transactions on Microwave Theory and Technique* **57**, 938–947.
11. **Worapishet A, Roopkom I and Surakampontorn W** (2010) Theory and bandwidth enhancement of cascaded double-stage distributed amplifiers. *IEEE Transactions on Circuits and Systems* **57**, 759–772.
12. **Amrani F, Trabelsi M, Youhami R and Aksas R** (2016) New design method of the single stage distributed amplifier. *Microelectronics Journal* **52**, 111–116.
13. **Alavi SA, Ghadirian S and Chabok S** (2017) Bandwidth and gain extension technique for CMOS distributed amplifiers using negative capacitance and resistance cell. *Microelectronics Journal* **60**, 60–64.
14. **Aitchison CS** (1985) The intrinsic noise figure of the MESFET distributed amplifier. *IEEE Transactions on Microwave Theory and Techniques* **33**, 460–466.
15. **Wu CT, Dong Y, Sun JS and Itoh T** (2012) Ring-resonator-inspired power recycling scheme for gain-enhanced distributed amplifier-based CRLH-transmission line leaky wave antennas. *IEEE Transactions on Microwave Theory and Techniques* **60**, 1027–1037.
16. **Mori K and Itoh T** (2008) *Distributed amplifier with CRLH-transmission line leaky wave antenna, Microwave Conference, EuMC 2008, 38th European, October*, pp. 686–689.
17. **Lai A, Itoh T and Caloz C** (2004) Composite right/left-handed transmission line metamaterials. *IEEE Microwave Magazine* **5**, 34–50.
18. **Moez K and Elmasry MI** (2006) Lumped-element analysis and design of CMOS distributed amplifiers with image impedance termination. *Microelectronics Journal* **37**, 1136–1145.
19. **Nikandish G and Medi A** (2014) Unilateralization of MMIC distributed amplifiers. *IEEE Transactions on Microwave Theory and Techniques* **62**, 3041–3052.
20. **Chenggang X** (2008) *Directional dual band distributed power amplifier with composite left/right-handed transmission lines, Microwave Symposium Digest, 2008 IEEE MTT-S International, June*, pp. 1135–1138.
21. **Mata-Contreras J and *et al.*** (2013) Design and experimental performance of diplexing MMIC distributed amplifier. *IEEE Microwave and Wireless Components Letters* **23**, 365–367.

APPENDIX A.

Eq. (11) can be written in a general form as follows:

$$\gamma = \sqrt{a + jb}, \tag{A.1}$$

The real and imaginary parts of (A.1) are obtained from (A.2a) and (A.2b).

$$\Re e(\gamma) = \alpha = \sqrt{\sqrt{a^2 + b^2}} \times \cos\left(0.5 \times \tan^{-1}\left(\frac{b}{a}\right)\right), \tag{A.2a}$$

$$\mathrm{Im}(\gamma) = \sqrt{\sqrt{a^2 + b^2}} \times \sin\left(0.5 \times \tan^{-1}\left(\frac{b}{a}\right)\right). \tag{A.2b}$$

According to (A.2a), α is minimized when

$$\tan^{-1}\left(\frac{b}{a}\right) \to \pi \Leftrightarrow \begin{cases} 1)\ a \to -\infty \\ 2)\ b \to 0 \quad \& \quad a < 0, \end{cases} \tag{A.3a}$$

and α is maximized when

$$\tan^{-1}\left(\frac{b}{a}\right) \to 0 \Leftrightarrow \begin{cases} 1)\ a \to +\infty \\ 2)\ b \to 0 \quad \& \quad a > 0 \\ 3)\ b \to +\infty \quad \& \quad a < 0. \end{cases} \tag{A.3b}$$

By comparing (11) and (A.1), it can be concluded that:

$$\begin{cases} a = \Re e\left(A \pm \sqrt{B + 4C}\right) \overset{\substack{A \text{ and } B \text{ are real} \\ C \text{ is complex}}}{\longrightarrow} a = A \pm \Re e\left(\sqrt{B + 4C}\right) \\ b = \mathrm{Im}\left(A \pm \sqrt{B + 4C}\right) \overset{\substack{A \text{ and } B \text{ are real} \\ C \text{ is complex}}}{\longrightarrow} b = \mathrm{Im}\left(\sqrt{B + 4C}\right). \end{cases} \tag{A.4}$$

Hence, (A.3a) and (A.3b) can be rewritten as follow:

$$\alpha_{\min} \Leftrightarrow A \pm \Re e\sqrt{B + 4C} < 0 \ \& \begin{cases} (1)\ A \pm \Re e(\sqrt{B + 4C}) \to -\infty \\ (2) \quad \text{or} \quad \mathrm{Im}(\sqrt{B + 4C}) \to 0 \end{cases} \tag{A.5a}$$

$$\alpha_{\max} \Leftrightarrow A \pm \Re e\sqrt{B + 4C} > 0 \ \& \begin{cases} (1)\ A \pm \Re e(\sqrt{B + 4C}) \to +\infty \\ (2) \quad or \quad \mathrm{Im}(\sqrt{B + 4C}) \to 0, \end{cases} \tag{A.5b}$$

$$\{(3)\ \mathrm{Im}(\sqrt{B + 4C}) \to +\infty \ \& A \pm \Re e(\sqrt{B + 4C}) < 0. \tag{A.5c}$$

These equations can be used to design the proposed CRLH TL with the minimum attenuation coefficients at an arbitrary frequency band. Note that, to simplify the analysis, "2" in (11) was removed because it has no effect on the analysis.

APPENDIX B

Finding the corresponding frequencies to α_{max}

In the case where $A \pm \Re e(\sqrt{B + 4C}) \to +\infty$

Equation (A.5b) shows that the attenuation coefficients are maximized when $A \pm \Re e(\sqrt{B + 4C}) \to +\infty$. As said previously, by using the conventional

https://doi.org/10.1017/S1759078718001265 Published online by Cambridge University Press

CRLH, $A \pm \Re e(\sqrt{B+4C})$ is always negative, but this situation is changed by using the proposed CRLH TL. As shown in Fig. 15, the terms "A" and $\Re e(\sqrt{B+4C})$ are always negative and positive, respectively. Using the proposed CRLH, "A" becomes positive, which can transform $A \pm \Re e(\sqrt{B+4C})$ to a positive value, when

$$A + \Re e(\sqrt{B+4C}) > 0 \rightarrow A > -\Re e(\sqrt{B+4C}) \Rightarrow \text{Great increment of } \alpha_1, \tag{B.1a}$$

$$A - \Re e(\sqrt{B+4C}) > 0 \rightarrow A > \Re e(\sqrt{B+4C}) \Rightarrow \text{Great increment of } \alpha_2. \tag{B.1b}$$

From Fig. 15, Equation (B.1a) is satisfied at frequencies higher than $\omega_{\alpha\ \min\ 3}$ = 12.8 GHz, limiting the bandwidth. But (B.1b) cannot be satisfied, and α_2 did not show a peak at the pole frequency $\omega_{\alpha\ \min\ 3}$, as is cleared in Fig. 10.

In the case where $\mathrm{Im}\sqrt{B+4C} \rightarrow +\infty$

According to (A.5c), α is maximized when $\mathrm{Im}\sqrt{B+4C} \rightarrow +\infty$ and $A \pm \Re e(\sqrt{B+4C}) < 0$. From Fig. 15, $A \pm \Re e(\sqrt{B+4C}) < 0$ is satisfied at frequencies lower than $\omega_{\alpha\ \min\ 3}$ = 12.8 GHz. In addition, from (A.2b), $\mathrm{Im}\sqrt{B_{new}+4C}$ becomes large when sin $(0.5 \tan^{-1}\ (4C/B_{new}))$ approaches one; therefore:

$$\mathrm{Im}\sqrt{B+4C} \rightarrow +\infty \Rightarrow \sin\left(0.5\tan^{-1}\frac{4C}{B_{new}}\right) \rightarrow 1 \Rightarrow \tan^{-1}\frac{4C}{B_{new}} \rightarrow \pi. \tag{B.2}$$

"B_{new}" can be obtained from (B.3):

$$B_{new} = \left((j^2\omega^2 L_g C'g) - \left(j\omega L_r + \frac{1}{j\omega C_l} \right) \times \left(\frac{1}{j\omega L_m + \frac{1}{j\omega C_r + (1/j\omega L_l)}} + j\omega C_{gd} \right) \right)^2. \tag{B.3}$$

According to (B.3) and selected element values for the designed circuit, term "B_{new}" is a positive real value; thus, (B.2) is not satisfied and max $(\tan^{-1}(4C/B_{new}))$ is equal to $\pm\pi/2$, which is established when $B_{new} = 0$. Finally, by equating term B_{new} to zero, six frequencies are obtained, but only two of them are acceptable, f_1 = 4 GHz, f_2 = 7 GHz, in which α is maximized, as is shown in Fig. 10.

$$B_{new} = 0 \Rightarrow \omega^6(C_l C_r C_{gd} L_l L_r l_m - C_l C_r C'_g L_l L_m L_g) - \omega^4(C_l C_r L_l L_r + C_l C_{gd} L'_l L_r + C_r C_{gd} L_l l_m - C_l C'_g L_g L'_l) + \omega^2(C_l L_r + C_r L_l + C_{gd} L'_l) - 1 = 0, \tag{B.4}$$

where $L'_l = L_m + L_l$.



Hamed shahraki received the B.Sc. degree in electrical engineering from University of Sistan and Baluchestan, Zahedan, Iran, in 2008, the M.S. degree in Electrical Engineering from Shiraz University of Technology, Shiraz, Iran, in 2012, and is currently working toward the Ph.D. degree at the Shahid Bahonar University of Kerman, Kerman, Iran. His research interests are MTM, RF/microwave circuits design. He is currently involved with microwave devices based on CRLH TL.



Ahmad hakimi received his B.Sc. degree in Electrical Engineering from Technical College of Shahid Bahonar University of Kerman, Kerman, Iran, in 1986. Using the scholarship granted by the Ministry of Higher Education of Iran and Istanbul Technical University (ITU) in 1987, he started studying his M.Sc. and Ph.D. degrees in the Faculty of Electrical and Electronic Engineering at the ITU and received his M.Sc. and Ph.D. degrees in 1990 and 1996, respectively. His research interests include design and analysis of nonlinear RF circuits, numerical analysis and advanced engineering mathematics, analog filter design, and linear integrated circuits. He is currently with the Scientific and Industrial Research Center, Kerman, Iran, and the Department of Electrical Engineering, Shahid Bahonar University of Kerman, Kerman, Iran.



Kambiz Afrooz received the B.Sc. degree from the Shahid Bahonar University of Kerman, Kerman, Iran, in 2005, the M.Sc. and Ph.D. degrees from the Amirkabir University of Technology (Tehran Polytechnic), Tehran, Iran, in 2007 and 2012, all in Electrical Engineering. In May 2011, he joined the CIMITEC group, University Autonoma de Barcelona (UAB), Barcelona, Spain, as a Visiting Student. He is currently an Associate Professor with the Electrical Engineering Department, Shahid Bahonar University of Kerman, Kerman, Iran. His research interests are in the areas of computer aided design of active and passive microwave devices and circuits, computational electromagnetic, modeling and simulation of high speed interconnects, metamaterial transmission lines, and substrate integrated waveguide structures. He is also the recipient of the Electrical Engineering Department Outstanding Student Award in 2007.



Mohammad Mahdi Pezhman received the B.Sc. degree in Electrical Engineering from the Shahid Bahonar University of Kerman, Kerman, Iran, in 2012. He received the M.Sc. degree in electrical engineering at the Kerman Graduate University of Technology, Kerman, Iran, in 2014. Now, he is the Ph.D. student of Yazd University and his research interests include design of RF building blocks for ultra-wideband amplifier and composite Right/handed transmission line. The focus of his research is on design of dual-band distributed amplifier (DBDA) with high gain and low power consumption.

https://doi.org/10.1017/S1759078718001265 Published online by Cambridge University Press